Formation of Dielectric Layers and Charge Regulation in Protein Adsorption at Biomimetic Interfaces

ARTICLE *in* LANGMUIR · DECEMBER 2011

Impact Factor: 4.46 · DOI: 10.1021/la204309a · Source: PubMed

5 AUTHORS, INCLUDING:

Rune Andersen Hartvig
University of Oslo
11 PUBLICATIONS **176** CITATIONS
SEE PROFILE

Marco van de Weert
University of Copenhagen
86 PUBLICATIONS **2,675** CITATIONS
SEE PROFILE

Lene Jorgensen
University of Copenhagen
43 PUBLICATIONS **865** CITATIONS
SEE PROFILE

Henrik Jensen
University of Copenhagen
88 PUBLICATIONS **1,858** CITATIONS
SEE PROFILE

Langmuir

Article

pubs.acs.org/Langmuir

Formation of Dielectric Layers and Charge Regulation in Protein Adsorption at Biomimetic Interfaces

Rune A. Hartvig, Marco van de Weert, Jesper Østergaard, Lene Jorgensen, and Henrik Jensen*

Department of Pharmaceutics and Analytical Chemistry, Faculty of Pharmaceutical Sciences, University of Copenhagen, Universitetsparken 2, DK-2100 Copenhagen, Denmark

Supporting Information

ABSTRACT: Protein charge is an important parameter in the understanding of protein interactions and function. Proteins are subject to dynamic charge regulation, that is, the influence of the local environment (such as charged interfaces and biopolymers) on protein charge. Charge regulation is governed by differences in the dielectric and electrostatic environment between adsorbed protein and the free protein in bulk solution. In this work protein charge regulation is addressed experimentally by employing electrochemistry at interfaces between two immiscible electrolyte solutions (ITIES) as well as theoretically by developing a new protein adsorption model at ITIES. Electrochemistry at ITIES is shown to be particularly well suited to study protein charge regulation as the adsorbed protein experiences a different dielectric environment compared to the bulk phase and the external control of the water/oil potential difference allows systematic studies on how potential induced ion gradients affect protein charge. The theoretical model incorporates all the features of the experimental system and specifically takes into account protein charge regulation at ITIES as well as the impact of the formation of dielectric layers on the experimentally observed impedance. The model parameters include the protein charge−pH profile, bulk pH, and the overall potential difference. It is shown that the formation of a dielectric layer and the associated charge regulation are the main factors dictating the observed experimental behavior. Finally, the theoretical model is used to interpret literature results, and the consistency between the model and the relatively large data set suggests that the model may be used more generally for understanding and predicting protein adsorption.

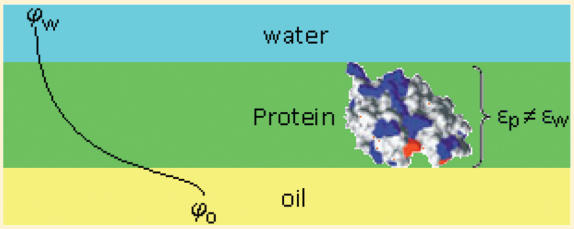

INTRODUCTION

Proteins are known to adsorb strongly to hydrophobic interfaces such as those found at cell membranes, emulsions, and the biomimetic oil−water interfaces employed in electrochemistry at the *interface between two immiscible electrolyte solutions* (ITIES).[1−4] In general, the formation of an interfacial layer has an influence on the conductive properties of the interfacial region and is therefore often termed a dielectric layer,[5,6] characterized by having a different relative permittivity than the bulk solution. Further, the proximity to other charged proteins in the layer and the ion gradient between the interface and the bulk solution has an impact on the potential profile across the layer. Therefore, ampholytes that are charged in bulk solution are not necessarily charged at the interface, and vice versa, since both the dielectric and electrostatic environment may result in charge regulation.[5,7−11] The fact that proteins at interfaces may not have the same charge as in the bulk solution has implications for interpretation of protein adsorption and for the understanding of proteins at interfaces in general.

Electrochemical capacitance measurement at ITIES is a very sensitive method to probe interfacial phenomena and offers the additional advantage of a fast and stable external control of the interfacial potential difference.[12−14] At the oil−water interface capacitance measurements have been used to detect and study adsorption of the proteins bovine serum albumin,[15] insulin,[16] hemoglobin,[17] lysozyme,[18] and glucose oxidase,[6,19] as well as the adsorption of phospholipids.[20−23] Protein adsorption at the ITIES also has an effect on the potential dependent transfer of smaller ions at the interface, which has been investigated for fast detection and characterization of proteins,[2,12,17,18,24−29] and, recently, the applicability to study protein unfolding at the interface has been demonstrated.[30]

Computational models to simulate electrochemical responses at the ITIES are based on the Verwey−Niessen model of the liquid−liquid interface, which is essentially an application of the Gouy−Chapmann theory derived for two back-to-back diffuse layers.[31−33] However, the interfacial behavior of large biomolecules, such as proteins, is complicated, and capacitance data are difficult to interpret. Theory and comparable experimental data are lacking; one of the goals of this work is therefore to qualify the interpretation of experimentally measured capacitance curves at the ITIES through development of a theoretical model for adsorption and capacitance. Specifically we investigate the formation of dielectric layers, potential dependent protein charge regulation, and the impact on observable capacitances. The experimental capacitances obtained in the present work are in good accordance with the

Received: November 3, 2011
Published: December 20, 2011

Scheme 1. Schematic Representation of the Electrochemical Cell Used

	Ref. phase	Oil Phase	Aqueous Phase	
Ag/AgCl	1 mM BTPPACl (Aq.)	5 mM BTPPATPFB (oil)	10 mM Phosphate Buffer + 1 mM NaCl ± Protein solution (Aq.)	Ag/AgCl

developed theory, suggesting that the developed model may be used as a more general approach to understand protein adsorption and charge regulation.

EXPERIMENTAL SECTION

Reagents. Deionized water (18.2 MΩ cm) was obtained from a Millipore Milli-Q system (Millipore, Bedford, MA). Succinic anhydride was from Aldrich-Chemie (Steinheim, Germany). Lysozyme, the organic solvent 1,2-dichloroethane (DCE), and the salt bis(triphenylphosphoranylidene)-ammonium chloride (BTPPACl) were obtained from Fluka Chemie (Buchs, Switzerland). The salt lithium tetrakis-(pentafluorophenyl)borate (LiTPFB) was obtained from Boulder Scientific Company (Mead, U.S.). The organic salt BTPPATPFB was prepared by metathesis of BTPPACl and LiTPFB as described elsewhere.[16]

Succinylation of Lysozyme. Lysozyme was reacted with succinic anhydride following the procedure by van der Veen et al.[34] Briefly, stock solution of 1.6 mM lysozyme in 10 mM phosphate buffer at pH 7.4 was allowed to react with a large surplus (more than 10:1 mol) of succinic anhydride added in small portions, and pH was continuously adjusted to 7.4 by adding NaOH. Succinic anhydride reacts with a protein on the N-terminus and lysine and tyrosine side groups to form a succinic acid group. The pK_a of succinic acid is approximately 4; thus, substitution with this group will shift the net protein charge to a negative charge at neutral pH. Succinic anhydride has a competing reaction with water to form free succinic acid, which is why a large excess must be added to the solution to ensure a complete reaction with the protein.

A control experiment was done to ensure that the capacitance response observed for succinyl-lysozyme was in fact due to the succinylated protein and not succinic acid formed by the side reaction of succinic anhydride with water in the preparation of succinyl-lysozyme: a solution was prepared by adding succininc anhydride to the buffer solution (without lysozyme) and continuously adjusting pH to 7.4. This solution was added to the electrochemical cell but was found not to affect the capacitance curves of the blank cell, demonstrating that adsorption of succinylated lysozyme is accountable for the observed responses.

Capacitance Measurements. Capacitance measurements were performed as previously described,[18] using a four electrode potentiostat PGSTAT30 (Autolab, Eco Chemie B.V., Utrecht, The Netherlands) and a custom-made glass cell from EuroGlas (Karlslunde, Denmark). The surface area of the organic−aqueous interface was 1.2 cm^2. The Galvani potential difference ($\Delta_o^w\varphi$) was controlled using two Ag/AgCl reference electrodes, one in the aqueous phase and one in a reference phase in contact with the oil phase (Scheme 1). The two counter electrodes were made of pure platinum and situated at each side of the interface.

All potentials are taken with point of reference in the aqueous phase, so that a positive potential corresponds to a more positive potential for the aqueous phase relative to the potential of the oil phase. The potential is adjusted to the Galvani potential scale by fixing the potential of zero charge (pzc) of the cell without protein at $\Delta_o^w\varphi = 0$.[35] Capacitance−potential curves were obtained by measuring the real and imaginary current response from a sinusoidal voltage amplitude of 5 mV (rms) and a frequency of 6 Hz at a range of potential values. In the absence of ion transfer across the interface, the total impedance can be considered as a resistor and capacitor in series. The interfacial capacitance (C) is then obtained as

$$C = \frac{1}{\omega \times Z_{Im}} \tag{1}$$

where Z_{Im} is the imaginary part of the impedance and ω is the angular frequency calculated as the applied frequency times 2π.

THEORETICAL BASIS

In this paper our previously developed phenomenological model of protein adsorption at charged liquid−solid interfaces[8] is reformulated to simulate proteins adsorbing at hydrophobic liquid−liquid interfaces. The presented model is solved numerically in Maple ver. 13, and the program file is available from the authors upon request.

Back-to-Back Diffuse Layer Model. The potential and the ion concentration near a charged interface differ from that in the bulk. The potential at the interface is the *surface potential* (φ_S) which depends on the potential difference, $\Delta_o^w\varphi = \varphi_w - \varphi_o$, between the bulk of the two phases and dielectric properties of the phases. The surface potential can be calculated from $\Delta_o^w\varphi$ by applying the electroneutrality condition to the *surface charge density* in the oil phase (σ_o) and the water phase (σ_w)

$$-\sigma_o = \sigma_w \tag{2}$$

which states that the excess charge on one side of the interface must be exactly matched by an opposing charge on the adjacent phase. The individual surface charge densities can be calculated from eqs 3 and 4 assuming a 1:1 electrolyte[31]

$$\sigma_w = -\sqrt{8RT\varepsilon_w\varepsilon_0 c_w}\sinh\left(\frac{F(\varphi_S)}{2RT}\right) \tag{3}$$

and

$$\sigma_o = -\sqrt{8RT\varepsilon_o\varepsilon_0 c_o}\sinh\left(\frac{F(\varphi_S + \Delta_o^w\varphi)}{2RT}\right) \tag{4}$$

where R, T, and F are the gas constant, the absolute temperature, and the Faraday constant, ε_o, ε_w, and ε_0 are the relative permittivities of the oil phase, water phase, and a vacuum, respectively, and c_o and c_w are the electrolyte

dx.doi.org/10.1021/la204309a | Langmuir 2012, 28, 1804−1815

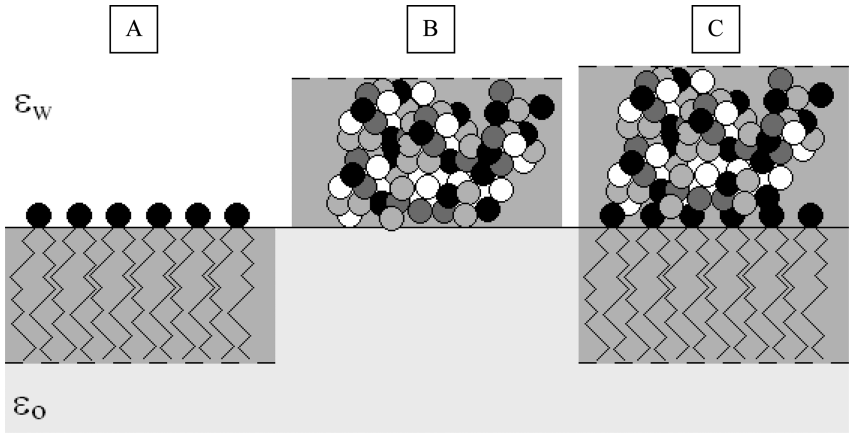

Figure 1. Formation of dielectric layers by proteins and lipids at the liquid−liquid interface. In the aqueous phase (top) the relative permittivity is that of water (ε_w), in the oil phase (bottom) that of the oil (ε_o), and inside the dark gray areas the relative permittivity may be different from the surrounding bulk phases depending on the dielectric properties of the adsorbed compound. (A) Lipid layer, (B) protein layer, and (C) mix, where a protein adsorbs to a lipid layer.

concentration of the respective phases. When they are connected through eq 2, the surface potential (φ_S) can be calculated.

Modification Incorporating Adsorption. Adsorption of a charged molecule at the interface will change the surface charge density in the phase where the charge is located. If, for example, a charged molecule adsorbs at the aqueous side of the interface the electroneutrality condition must apply, and the charge density on the aqueous side now consists of the contribution from the adsorbate molecules (σ_{ads}) and the distributed ions (σ_w):

$$-\sigma_o = \sigma_w + \sigma_{ads} \tag{5}$$

The charge contributed by adsorption may be calculated from the effective net charge of the adsorbate (Z_{net}) at the interface, the Faraday number (F), the maximum surface coverage (Γ_{max}), and the fractional coverage (θ):[31]

$$\sigma_{ads} = z_{net}\cdot F\cdot\Gamma_{max}\cdot\theta \tag{6}$$

A potential dependent Langmuir isotherm may be used to describe adsorption at charged interfaces[8]

$$\theta = \frac{c_p\cdot\exp\left(-\frac{\Delta G^0_{ads}(\text{chem})}{RT}\right)\cdot\exp\left(-\frac{z_{ads}F\varphi_S}{RT}\right)}{1 + c_p\cdot\exp\left(-\frac{\Delta G^0_{ads}(\text{chem})}{RT}\right)\cdot\exp\left(-\frac{z_{ads}F\varphi_S}{RT}\right)} \tag{7}$$

where c_p is the concentration of the free adsorbate molecule, $\Delta G^0_{ads}(\text{chem})$ is the contribution to the total free energy of adsorption from all other forces than electrostatics, and the electrostatic contribution is given by the term $Z_{ads}F\varphi_S$, where Z_{ads} represent the charge of the molecule that interacts with the surface. For large molecules, such as proteins, where not all charges interact equally strong with the surface and surface orientation of the protein would have to be considered, this charge should be distinguished from the net charge Z_{net} in eq 6. For a small molecule, the net charge is assumed to be at the surface and $Z_{ads} = Z_{net}$. Some special cases may arise that complicate or simplify eq 7; for example, (1) the concentration may be substituted with a mass balance equation in cases that take into account bulk phase depletion of the adsorbate,[8] or (2) in cases of strong and potential independent adsorption, when $\Delta G^0_{ads}(\text{chem}) \ll 0$, the fractional coverage (θ) simplifies to a value of 1. This situation may occur for proteins adsorbed at a hydrophobic interface such as the ITIES. Since the electrostatic interaction energy is of relatively low importance, it is not as important to consider a surface orientation of the protein at the hydrophobic oil−water interface, as it is on a hydrophilic surface.[8]

In any case, substituting eqs 3, 4, 7, and 6 into eq 5 a relation between the potential difference ($\Delta^w_o\varphi$) and the surface potential (φ_S) is obtained. This system of equations can be solved numerically for known values of $\Delta^w_o\varphi$ to obtain corresponding φ_S values. The calculated φ_S can then be used to calculate, e.g., the surface charge densities in the two phases, eqs 3 and 4, or of the adsorbate, eq 6, and the potential distribution in solution (Supporting Information, equation S6), as described in the literature with more details for liquid−liquid[31] and liquid−solid interfaces.[8] The following subsections present a new model, by considering the possibility of the adsorbed layer to change the relative permittivity at the surface and by considering charge regulation in these layers.

Dielectric Layers. The calculation of the electrolyte charge density using eqs 3 and 4 can be modified by considering the formation of a dielectric layer upon adsorption. For instance, lipids extrude their hydrophobic carbon tail into the oil phase creating a layer of nanometer thickness (Figure 1A) with an estimated relative permittivity, $\varepsilon_d = 2$.[20] Likewise, protein adsorbed at the aqueous side may form a layer with a lower relative permittivity than water (Figure 1B), or a mix of the two situations can be envisioned when, e.g., a protein adsorbs at a lipid layer at the oil−water interface (Figure 1C).

The change of dielectric properties with adsorption is incorporated in eqs 3 and 4 by replacing the relative permittivity of water (ε_w) and oil (ε_o) with an effective relative permittivity, which is a function of the pure phase permittivities (ε_o or ε_w), the permittivity of the dielectric layer (ε_d), and the surface coverage (θ):

$$\varepsilon_{o,eff} = \varepsilon_o\cdot(1-\theta) + \varepsilon_d\cdot\theta \tag{8a}$$

$$\varepsilon_{w,eff} = \varepsilon_w\cdot(1-\theta) + \varepsilon_d\cdot\theta \tag{8b}$$

dx.doi.org/10.1021/la204309a | Langmuir 2012, 28, 1804−1815

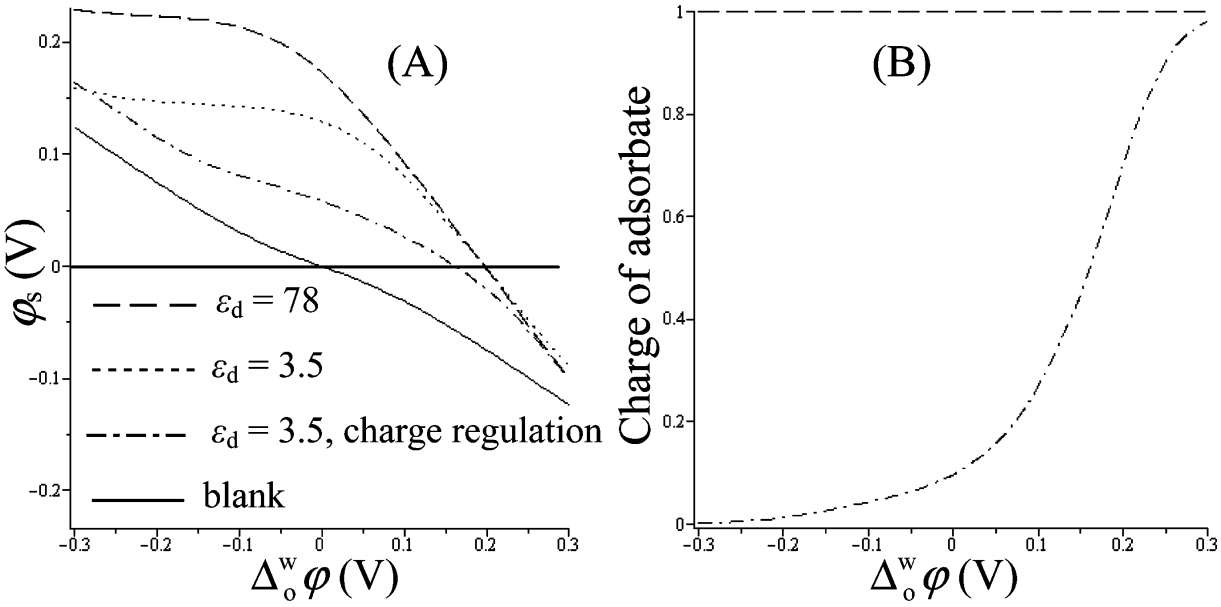

Figure 2. Without adsorption (solid), with no dielectric layer (dash), dielectric layer (dot), and with dielectric layer and charge regulation (dash dot). (A) Surface potential (φ_S) as a function of potential difference. (B) Net charge of the adsorbate as a function of potential difference. The net charge is a constant +1 except when considering charge regulation. In both (A) and (B) the following conditions are used: $z_{ads} = z_{net} = 1$, $\theta = 1$, $\Gamma_{max} = 1{\cdot}10^{-6}$ mol·m^{-2}, $c_w = c_o = 10$ mM. In the simulation that considers charge regulation (dash dot) pH = pK_a = 7.0, in the absence of charge regulation the charge is independent of pH.

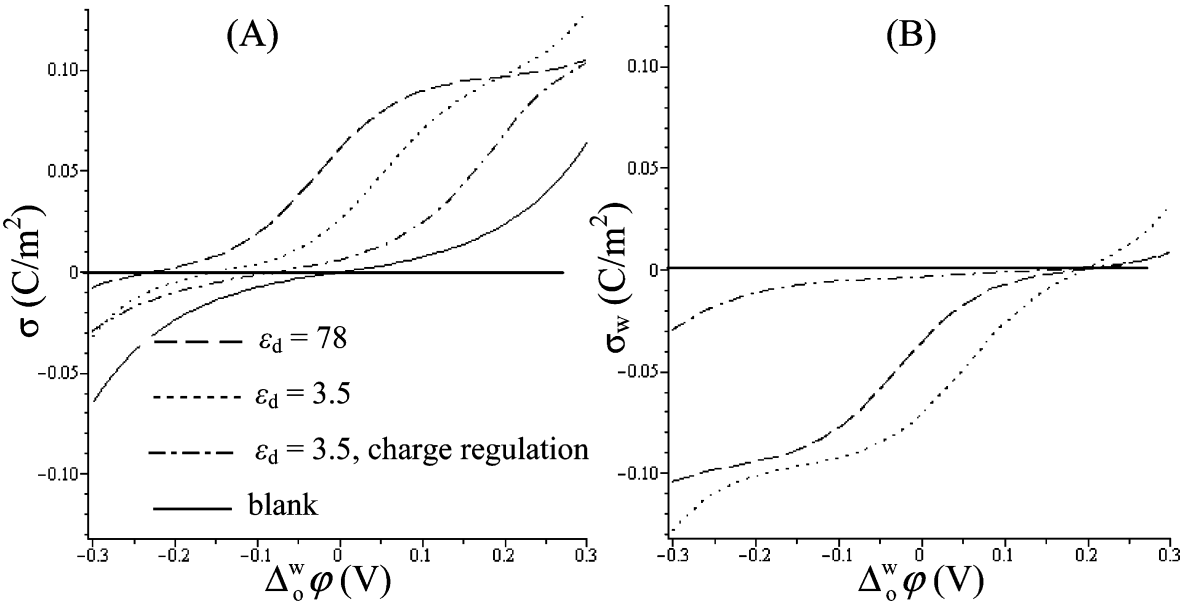

Figure 3. (A) Surface charge density of the interfacial region, $\sigma = -\sigma_o = \sigma_w + \sigma_{ads}$. (B) Surface charge density of the aqueous electrolyte σ_w. In (A) and (B) the simulation parameters are the same as in Figure 2.

The dielectric layer only exists in the surface region, and ideally the dielectric properties of the bulk phase beyond the layer could be considered by including some distance dependence.[6,36,37] Further, if adsorption is strong (θ = 1), the effective relative permittivity of the relevant interfacial region equals that of the adsorbate ($\varepsilon_{eff} = \varepsilon_d$).

Charge Regulation. The charge of an ampholyte should not be considered a constant value as it is highly influenced by the local electrostatic environment. Consequently, large differences may therefore be observed between bulk and adsorbed protein charge state. Two major factors are recognized to explain this; a change in the local potential and a difference in the dielectric environment.[38] In the Supporting Information it is shown how the effect of the local potential is calculated from the usual Gouy−Chapmann equation and how the effect of the relative permittivity on apparent pK_a is calculated on the basis of literature data[38] (Figure S1 in the Supporting Information). For a small molecule adsorbed at an interface, the calculation is straightforward and involves the relative permittivity of the interface and the surface potential. The polarity of the interface is calculated from the polarity of the bulk phases as a simple average.[39] As a measure of polarity the $E_T(30)$ polarity scale is used, where values for water and DCE can be found in the literature.[40] The average $E_T(30)$

dx.doi.org/10.1021/la204309a | *Langmuir* 2012, 28, 1804−1815

polarity value is then translated to a relative permittivity of the interface by the equation given by Iwunze,[41] and further translated to a shift in apparent pK_a from Figure S1. In this way the relative permittivity of the DCE–water interface was calculated to be ε = 25, resulting in a difference between bulk phase pK_a and apparent pK_a of $|\Delta pK_a|$ = 1.5 (Figure S1). The influence of surface potential on the charge of the small molecule is calculated directly from the Gouy–Chapmann theory (equation S2).

For an adsorbed protein some amino acids are located at the interface, and charge regulation for these amino acids is treated as the small molecule discussed above. Other amino acids are located at a distance from the interface within an adsorbed layer. The relative permittivity used for the calculation of the charge residing on these groups is based on an estimation of the relative permittivity inside the protein layer.

Differential Capacitance. The differential capacitance is calculated as the derivative of the surface charge density:[31,42]

$$\frac{1}{C_d} = \frac{d\Delta_o^w\varphi}{d\sigma} = \frac{1}{C_w} + \frac{1}{C_o} \tag{9}$$

The differential capacitance on each side of the interface is given by

$$C_w = -\frac{d(\sigma_w + \sigma_{ads})}{d(\varphi_S)} \tag{10}$$

and

$$C_o = -\frac{d\sigma_o}{d(\varphi_S + \Delta_o^w\varphi)} \tag{11}$$

The differential capacitance depends on the accumulative excess charge in the whole interfacial region (diffuse layer in both phases), not just directly at the surface. When, e.g., a protein adsorbs, the net charge on the protein changes the charge in the interfacial region which is why, in an experimental setting, a change in capacitance is an indication of adsorption.

RESULTS AND DISCUSSION

Effect of Adsorption on Interfacial Properties. The effects of dielectric layers and charge regulation on interfacial parameters can be described by considering a generalized molecule with charge z = +1, θ = 1, and $\Gamma_{max} = 1 \times 10^{-6}$ mol·m^{-2}. The results in Figure 2, Figure 3, and Figure 4 represent results from the same simulation. The system of equations (eqs 2–6) is solved numerically at different applied water/oil potential differences ($\Delta_o^w\varphi$), to obtain the surface potential, φ_S, as shown in Figure 2A. The simulations illustrate the effect of adsorption, with (dots) or without (dashed line) formation of a dielectric layer in the aqueous phase, and the effect of charge regulation (dash dot) compared to the situation without adsorption (solid line). In the dielectric layer simulation a value of ε_d = 3.5 is used since this is close to the values often used in simulation for proteins.[43] In the simulation considering charge regulation a dielectric layer is also assumed, and the apparent pK_a value of the +1 group is chosen to be the same as the pH (Figure 2B).

The surface potential is an important property in describing adsorption and charge regulation at the interface. In the absence of adsorption, the surface potential, φ_S, is a simple function of the potential difference across the interface, $\Delta_o^w\varphi$, and the surface potential changes sign at $\Delta_o^w\varphi$ = 0 (Figure 2A, blank). However, the specific adsorption of the positively charged particle leads to a more positive surface potential, which then repels adsorbate in a negative feedback mechanism. This is, however, compensated for by charge regulation, which lowers the partial charge of the positive particle near a positive surface potential (Figure 2B). In the presence of adsorption it is observed that a large positive potential difference is required for the surface potential to become neutral (intersection with x-axis). The surface potential can be used to evaluate the surface charge density, σ (Figure 3A), which can be separated into the charge density of the background electrolyte, σ_w (Figure 3B), and charge density of the adsorbate (σ_{ads}).

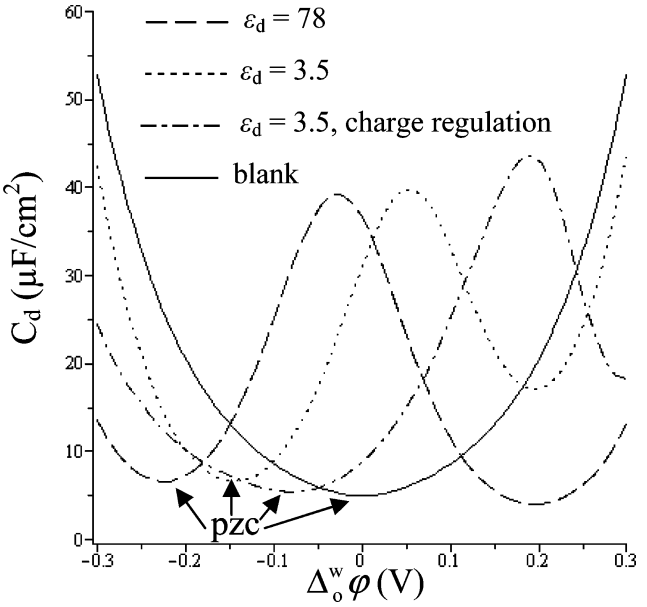

Figure 4. Potential of zero charge (pzc) is found at negative potentials, as expected for an adsorbed positive charge at the interface and as can be verified from the surface charge densities of the simulation (Figure 3A). The simulation parameters are the same as in Figure 2.

In the absence of adsorption the surface charge density (Figure 3A), which is the excess charge in the diffuse layer, is negative at $\Delta_o^w\varphi$ < 0, since the anions of the electrolyte are distributed in the solution in order to compensate the positive surface charge (Figure 2A). The intersection with the x-axis is at $\Delta_o^w\varphi$ = 0, and at $\Delta_o^w\varphi$ > 0 the surface charge density is positive as cations will be in excess in the diffuse layer at a negative interface potential. The adsorption of the positive ion causes an excess of positive charge in a larger part of the potential window, which is compensated by the background electrolyte at more negative potential differences. The potential where the excess charge in the diffuse layer is zero is identified as the "potential of zero charge" (pzc) and is observed as the intersection of the charge density curves with the x-axis (Figure 3A). The observed effect of the dielectric layer is that a higher potential difference ($\Delta_o^w\varphi$) is required to compensate the adsorbed charge. On the other hand, charge regulation decreases the effect by inducing a lower charge on the adsorbate resulting in a lower surface charge to be compensated. At more positive potentials the charge density of the aqueous electrolyte (σ_w) goes to zero (Figure 3B) as the charge of adsorbed molecules (σ_{ads}) completely balances the interfacial charge (σ).

The experimental obtainable parameter of the interface is the capacitance, which mathematically is the first derivative of the

dx.doi.org/10.1021/la204309a | Langmuir 2012, 28, 1804–1815

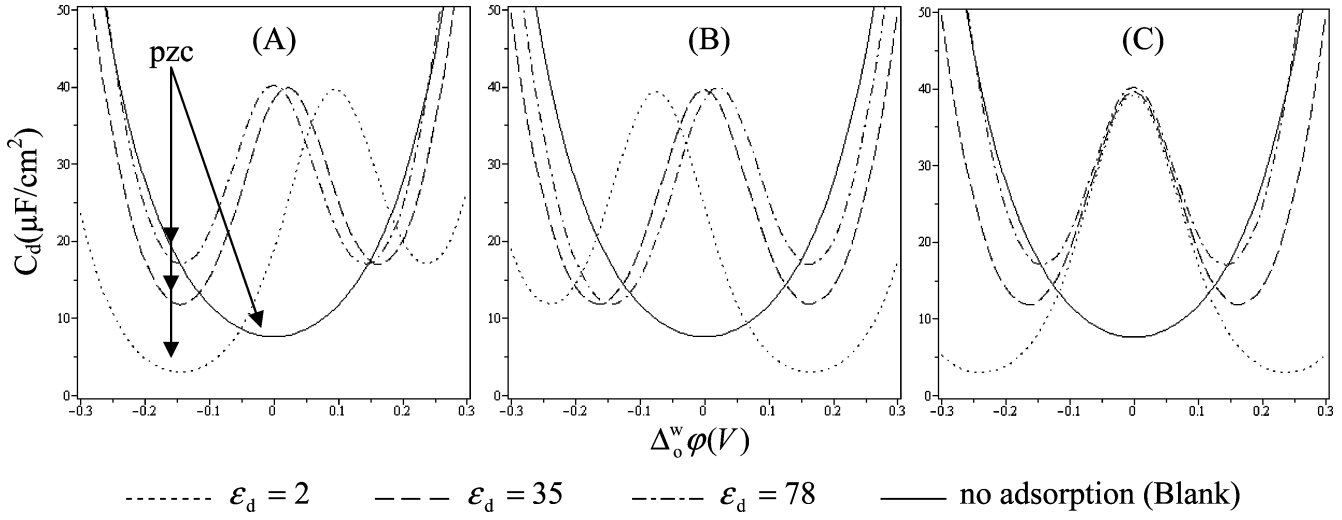

Figure 5. Influence of an adsorption dielectric layer on capacitance profiles if the dielectric layer is formed at (A) the oil side, (B) the aqueous side, or (C) both sides (see also Figure 1). A particle of charge +1 adsorbs strongly ($\theta = 1$) on a water ($\varepsilon_w = 78$)−nitrobenzene ($\varepsilon_o = 35$) interface. $\Gamma_{max} = 1{\cdot}10^{-6}$ mol·m^{-2}, $c_w = c_o = 10$ mM. The pH is not a simulation parameter as a permanent charge is assumed.

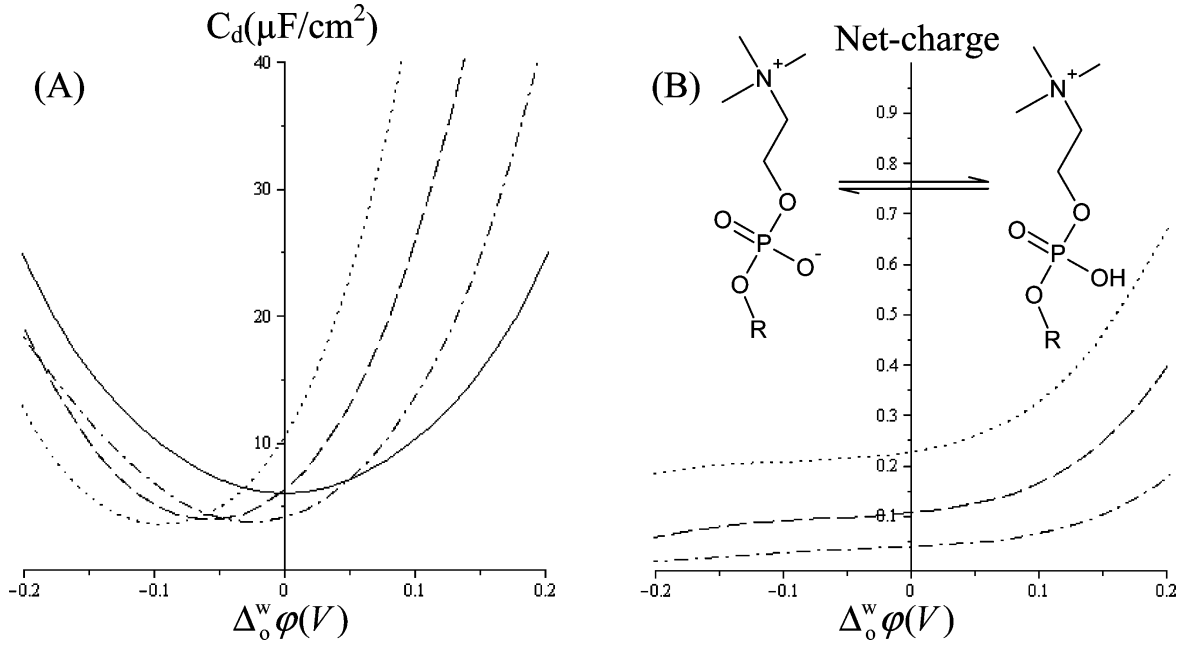

Figure 6. Charge regulation of the phosphate group in phosphatidylcholine as a function of potential difference. (A) Capacitance of the interface and (B) net charge of the lipid at the interface. At negative potential differences the phospholipid is adsorbed as a zwitterion, and at positive potential difference as a cation. The curves represent different bulk pH values of 2 (dot), 3 (dash), and 4 (dot dash). The solid curve corresponds to the blank interface. The apparent pK_a value used for the phosphate group was 3, and the pK_a for the quaternary ammonium is too extreme to be considered. In (A) and (B) the following conditions are used: $z_{ads} = z_{net}$, $\theta = 1$, $\Gamma_{max} = 1{\cdot}10^{-6}$ mol·m^{-2}, $c_w = c_o = 10$ mM.

surface charge density. The capacitance curves simulated for the above system are presented in Figure 4.

The strong adsorption of a charged particle changes the capacitance in the entire potential window. The potential of zero charge is seen to shift to negative potentials as was discussed from the intersection with zero in the surface charge density curves (Figure 3A). A large effect is also seen in the form of a capacitance peak. Such a peak is not usually observed in experiments and therefore requires further explanation. The observed effect of both a dielectric layer and charge regulation is to move the capacitance peak out of the potential window (Figure 4). Another factor displacing the peak is that the specific adsorption energy (ΔG^0_{ads}(chem)) is assumed to be large enough that maximum coverage is obtained in the whole potential window, whereas with falling ΔG^0_{ads}(chem) the peak is displaced outside the potential window.[31] In experiments, to avoid interference from transfer of background electrolytes, the capacitance is usually measured at potentials near the potential of zero charge (pzc), which is considered to coincide with the minimum of the capacitance curve (Figure 4). In summary, only one minimum is usually observed experimentally, and the peak is at most observed as a shoulder. The peak size is strongly dependent on the charge density of the adsorbate, which depends on the adsorption isotherm, net charge, and maximum surface coverage of the molecule.

dx.doi.org/10.1021/la204309a | *Langmuir* 2012, 28, 1804−1815

Effect of a Dielectric Layer on the Potential of Zero Charge. Figure 5 shows the effect on the capacitance, in the absence of electrostatic charge regulation, but assuming the formation of a dielectric layer upon adsorption in the different situations A, B, and C, corresponding to the illustrations in Figure 1: the formation of a dielectric layer in the oil phase (Figure 5A), the formation of a dielectric layer on the aqueous side (Figure 5B), or a mix of these situations (Figure 5C). It is seen that the curve is shifted to the left (negative potentials) upon adsorption of the positive ion, which is as expected. However, the nature of the dielectric layer has some noticeable effects in all of these situations, as discussed for the following limiting situations.

Case A. Compounds that could be expected to form a dielectric layer in the oil phase include lipids, surfactants, and membrane proteins. In Figure 5 with the decrease in relative permittivity of the oil phase near the interface it is observed that the capacitance curve is shifted to lower values. At $\varepsilon = 2$, which corresponds to the commonly given value of a lipid hydrocarbon tail, the minimum of the capacitance has fallen significantly below that of the blank interface. This is in good agreement with the experimental behavior of lipids, and formation of a dielectric layer is also usually suggested in the literature.[6,20−22,44] It should be noted that in the simulations the oil phase has $\varepsilon_o = 35$, corresponding to nitrobenzene; if ε_o is lower, e.g., 10 as for 1,2-dichloroethane (DCE), the difference between the pzc of the blank interface and dielectric layer will be less obvious. This is in agreement with, for example, the observed shift in pzc upon addition of phosphatidylcholine at a water−nitrobenzene interface compared to a similar adsorption at a water−DCE interface.[6,21]

Case B. Particles capable of forming a dielectric layer that exclusively exist at the aqueous side of the interface upon adsorption include peptides, proteins, and polymers. A relative permittivity for proteins of $\varepsilon = 3.5$ has been suggested and is often used in calculations and simulations.[43] This is low relative to the aqueous phase and suggests a large effect of a dielectric layer. The lower the relative permittivity, the farther away the pzc of the adsorbed layer will be from the pzc of the blank interface.

Case C. The situation depicted in Figure 1C shows a protein adsorbed on a lipid layer creating two dielectric layers, one in each phase.[6] This situation is not investigated further in this work but may be simulated using the developed model.

Effect of Adsorption of Lipids on Differential Capacitance (Case A). The lipid phosphatidylcholine has previously been suggested to adsorb by a charge regulation mechanism at low pH.[20] Figure 6 shows the expected capacitance curve and formal charge of the phospholipid at the interface. The bulk pK_a value of the phosphate group is ∼1.5, which is relatively far from the pH values investigated. However, as described in the theory section, solvation effects at the interface may result in an apparent interface pK_a different from the bulk phase value. At the DCE−water interface a shift to a pK_a value of 3 is thus predicted (see theory), and the phospholipid may therefore be charged at the interface. If we add the charge regulation effect from the potential difference, we see that as the potential difference increases to more positive values the phospholipid becomes overall positively charged due to protonation of the phosphate group at the interface. This explains why the zwitterions, which are neutral in the bulk solution, can adsorb as a positive ion at the electrified interface.[20] It should be noted that phosphatidylcholine may also adsorb as a positive ion at higher pH values, an observation that has been explained by the coadsorption of cations with the phosphate group.[45] However, the affinity of the phosphate group is higher for the proton than for cations; at low pH values the former equilibrium will therefore dominate.

This example shows that a molecule can change its overall charge with adsorption mediated charge regulation. It also demonstrates that charge regulation can increase the range of potential differences in which a given molecule adsorbs; at negative potential differences, where the surface potential is more positive, the cationic form of the phospholipid exists at the interface, whereas at positive potentials it shifts to a neutral form and thereby minimizes repulsion. As a result the phospholipid adsorbs relatively strong in the whole range of potentials. Figure 6B also shows that the phospholipid is primarily in the neutral form for most of the applied potential differences; this is because the accumulation of the charged adsorbate in itself changes the potential at the surface so that the potential experienced at the interface is not directly connected to the potential difference given on the x-axis. To recognize this, observe that at a potential difference of $\Delta_o^w\varphi = 0$ V, the neutral form is favored despite the pH value being equal to or less than the pK_a. This observation is caused by the adsorbed positive charges which by themselves result in charge regulation. We previously suggested a similar mechanism of charge regulation for proteins adsorbing at charged solid interfaces.[8]

Effect of Adsorption of Proteins on Differential Capacitance at ITIES (Case B). Proteins readily adsorb and form films at oil−water interfaces as is known from measurements based on, e.g., surface tension,[46] surface rheology,[3] and capacitance (see Table 1). It is generally accepted that proteins will adsorb at hydrophobic interfaces driven by a hydrophobic interaction and that electrostatic

Table 1. Proteins Investigated with Capacitance Measurements at the ITIES

protein	pH	pI	charge	shift of observed minimum	structural stability (ΔG_{den})[a]
Capacitance Data from Literature					
lysozyme[18]	2.8	12	+	−	hard (44 kJ/mol)[60]
glucose oxidase[19]	7	4.44	−	−	soft (6.7 kJ/mol)[61]
insulin[16]	7.4	5.4	−	−	soft (N/A)[c]
bovine serum albumin[15]	7.4	4−5	−	−	soft (15.6 kJ/mol)[62]
hemoglobin[17]	2	7	+	−	soft (N/A)[c]
Capacitance Data from This Work					
lysozyme	7.4	12	+	−	hard (61 kJ/mol)[60]
succinyl-lysozyme	7.4	4	−	+	hard (N/A)[b]

[a]Data chosen from studies with close to similar conditions as in the capacitance measurements as possible (pH, ionic strength, additives, etc.). [b]The structural stability of succinyl-lysozyme was investigated in a comparative study with lysozyme and concluded to have a lower stability than the unmodified protein but could still be characterized as a structurally stable (hard) protein at neutral pH.[34,59] [c]Insulin and hemoglobin are usually considered to be soft proteins, but relevant calorimetry data was not found for these proteins, so the classification here is with the reservation that proteins can have varying stability depending on conditions.

dx.doi.org/10.1021/la204309a | Langmuir 2012, 28, 1804−1815

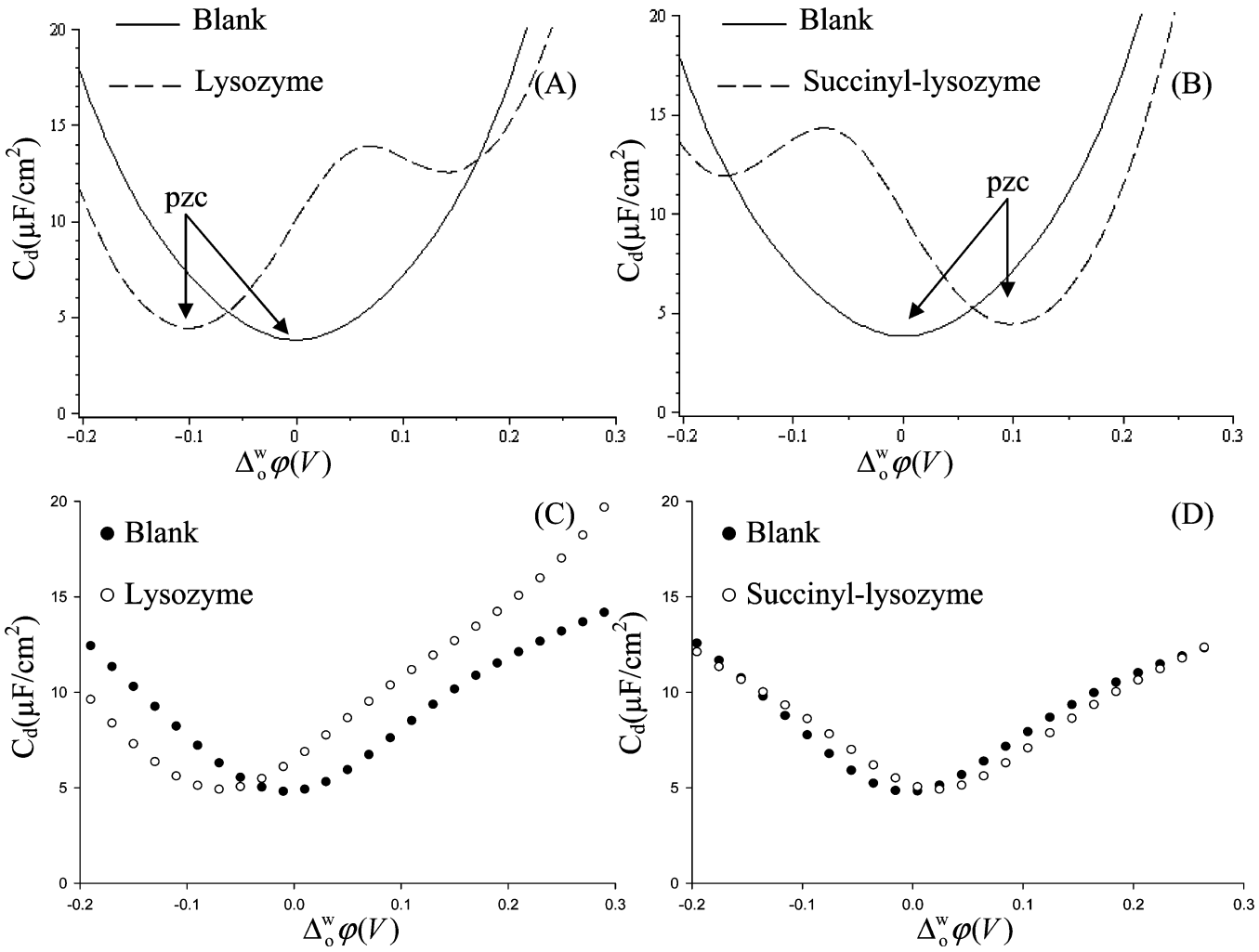

Figure 7. (A) Simulation of lysozyme (positively charged) and (B) succinyl-lysozyme (negatively charged). In (A) and (B) the conditions used are θ = 1, Γ_{max} = 4.4·10^{-8} mol·m^{-2}, c_w = 10 mM, and c_o = 5 mM. (C) Experimental capacitance curve of adsorption at 25 °C, pH = 7.4, and 25 μM lysozyme and (D) 25 μM succinylated lysozyme. Full coverage is reached at these concentrations; allowing longer equilibration time or adding more protein does not affect the capacitance curves.

interactions at such interfaces are of low importance.[47,48] Further, observations have led to a classification of proteins into "soft" and "hard" proteins, where soft proteins are less structurally stable in bulk solution than hard, as measured, for example, by differential scanning calorimetry.[47,48] Many observed characteristics of adsorbed protein layers are linked to this internal stability, and significant differences are observed in the mechanical and physical properties of adsorbed protein layers of soft and hard proteins at liquid interfaces.[46,49]

Neutron reflectivity and X-ray studies at air−water and oil−water interfaces show that proteins form a compact inner layer containing 80−90% of the amino acids at the interface and a less dense outer layer consisting of groups pointing out in solution, whereas only a small fraction is penetrating into the hydrophobic phase.[50−53] Despite a large difference in size, the structurally unstable protein β-casein (23.5 kDa) and bovine serum albumin (66.5 kDa) both form an inner layer of ca. 1 nm thickness, with the highest density at ca. 0.5 nm from the interface.[50,52,53] The more stable proteins lysozyme and β-lactoglobulin form thicker inner layers, 1.5−2 nm, with a maximum density at ca. 1 nm.[50,51] The compact layer thickness is lower than expected from the diameter of the native structure of the proteins pointing to some extent of unfolding of their tertiary structure at the interface. Martin et al. reported a correlation between structural stability and rheological properties of interfacial protein films by showing that soft proteins form more viscous films, while hard proteins films form more elastic films.[49] The structural and mechanical differences observed for layers formed by proteins with differing structural stability may also be reflected in differences in the relative permittivity of the layer. This property, which has a large influence on differential capacitance, is estimated from literature data[54] of poly lysine as a model of a soft protein and cytochrome c, which is structurally stable. The capacitance at a hydrophobic membrane was measured,[54] with or without a poly lysine layer, to find the ratio of layer thickness to relative permittivity, d/ε_d = 0.08 nm; from the measured value of the layer thickness the relative permittivity was calculated in the literature to be ε_d = 3.8.[54] This is remarkably close to the theoretical value of the relative permittivity, ε_d = 3.5, for a folded protein interior.[43] For cytochrome c a ratio, d/ε_d = 0.07 nm, was found, but the layer thickness was not measured. However, the layer thickness of this protein adsorbed at a hydrophobic interface is elsewhere measured to be 2.3 nm,[55] which is consistent with the layer thickness from X-ray and neutron reflectivity of hard proteins discussed above. We

dx.doi.org/10.1021/la204309a | Langmuir 2012, 28, 1804−1815

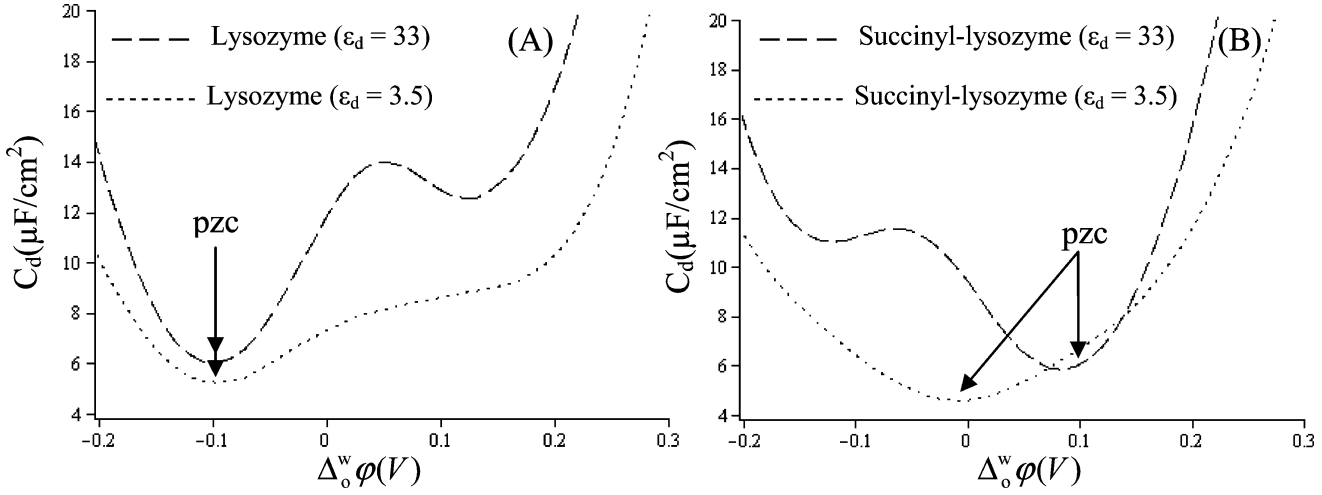

Figure 8. Simulation of (A) lysozyme and (B) succinyl-lysozyme as hard (ε_d = 33) and soft (ε_d = 3.5) proteins at the interface. Other conditions are θ = 1, Γ_{max} = 4.4·10^{-8} mol·m^{-2}, c_w = 10 mM, and c_o = 10 mM.

therefore estimate the dielectric layer of a hard protein to have a relative permittivity ε_d = 2.3/0.07 = 33.

Adsorption of Lysozyme and Succinyl-Lysozyme. From the above discussion, we expect the structurally stable proteins lysozyme and succinyl-lysozyme to adsorb at the aqueous side of the ITIES forming a dielectric layer (Figure 1B) with a relative permittivity of approximately ε_d = 33 and with amino acids in a compact layer on an average distance d = 1 nm from the interface. The effect of electric potential on the apparent pK_a of the amino acids in the dielectric layer is therefore calculated from the potential at this distance (see equation S3). Apparent pK_a values are calculated by correcting their bulk phase value for dielectric and electrical potential effects (Supporting Information). The uncorrected pK_a values are taken from literature data.[56] Further, we assume full coverage in the entire potential window, θ = 1, and the maximum surface concentration is found from experimental values on a hydrophobic surface to be Γ_{max} = 4.4·10^{-8} mol/m^2.[57] Results of the simulation are shown in Figure 7A and Figure 7B. The observed global minimum for the simulated curves is identical to the potential of zero charge (pzc) as can be verified from the simulated surface charge density curves (data not shown). As expected for an adsorbing positive charge, lysozyme shifts the pzc to more negative potentials. Likewise, succinyl-lysozyme shifts the pzc to more positive potentials as expected for a negative charge. Since we have assumed maximum surface coverage at all potentials the capacitance curve of the proteins differs from the blank curve in the entire potential range; this corresponds with published capacitance data of proteins at the ITIES (e.g., see references in Table 1). The corresponding experimental differential capacitance curves for lysozyme and succinylated lysozyme are shown in Figure 7C and Figure 7D. The experimental parameters are the same as in the simulation, c_w = c_o = 10 mM, T = 25 °C, c_p = 25 μM, and pH = 7.4.

To verify that the experiments represent maximal covered protein layers as assumed, the protein concentration is increased by adding more stock solution. The fact that this does not further affect the measured capacitance curve (data not shown) confirms that maximum surface coverage of both proteins is reached at all potentials. The simulation (Figure 7A and Figure 7B) qualitatively describes the observed capacitance for both proteins; i.e., both the shift in pzc and the general shape of the capacitance curve are reproduced. However, for both proteins the observed shift in pzc in the experiment is smaller than in the simulation, and the curve of the capacitance near the pzc is steeper in the simulation. The relative steepness of the simulated capacitance curve is a well-known artifact of the Gouy−Chapmann model, originating from the model's treatment of ions as point charges.[58] Though full coverage is reached and capacitance is found to change at all potentials, the change observed is smaller for succinyl-lysozyme. In the model this can be explained if the amount of charge brought to the surface per molecule of adsorbed succinyl-lysozyme is smaller than per lysozyme molecule. Physically this is plausible since succinyl-lysozyme (1) is larger due to succinylation, (2) probably denatures to a larger extent than lysozyme,[34,59] and (3) is more sensitive to charge regulation, from both the surface and the protein layer, since the pK_a of the succinyl group is closer to the pH in the experiment compared to the positively charged amino acids that it has substituted on lysozyme (mostly lysine).

As discussed, the experimental results obtained here are in accordance with theory in that a shift to more negative potential values are observed for the capacitance curve of the positive lysozyme, and a shift to more positive values for the negatively charged succinyl-lysozyme. However, the capacitance curves reported for a number of proteins show a shift opposite of that expected based on bulk phase net charge as summarized in Table 1.

It may be noted that the results for succinyl-lysozyme represent the first reported shift of the capacitance curve to more positive potentials for a protein. Note also that the proteins which have a shift in pzc opposite of expectations based on net charge are proteins with a limited structural stability (soft proteins). As discussed earlier, physical properties of adsorbed layers of structurally labile proteins may differ significantly from stable proteins such as lysozyme and succinyl-lysozyme. Specifically, the more viscous layer formed by soft proteins is expected to have a much lower relative permittivity.

Differential Capacitance of Soft Proteins. To investigate the model's prediction of the behavior of soft proteins, adsorption of lysozyme and succinyl-lysozyme were simulated with a relative permittivity of the layer equal to 3.5 (Figure 8).

For lysozyme the capacitance curve still exhibits a shift to more negative potentials, while soft succinyl-lysozyme now also

dx.doi.org/10.1021/la204309a | Langmuir 2012, 28, 1804−1815

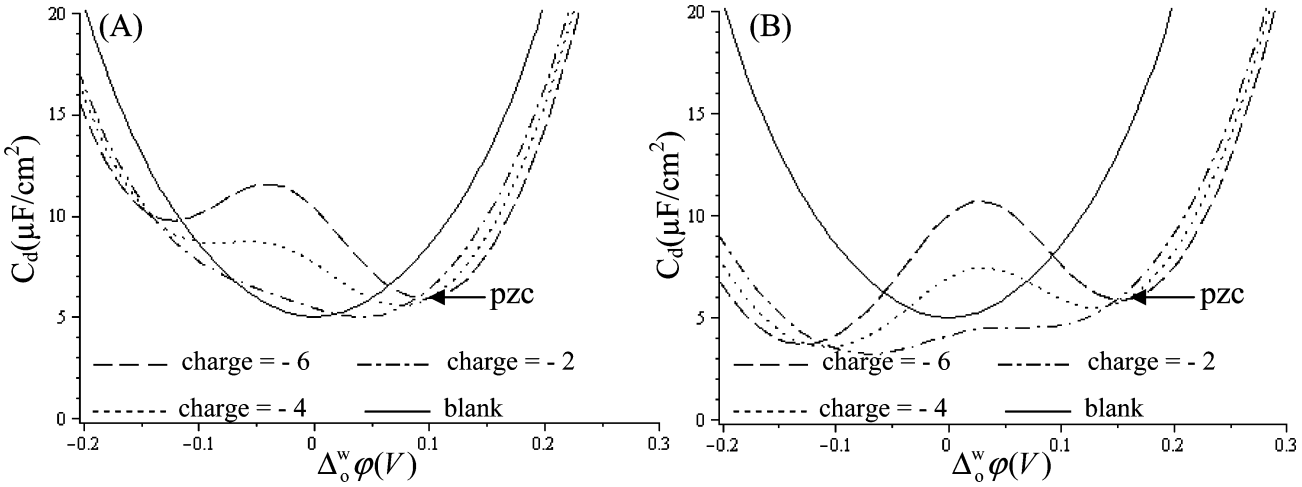

Figure 9. Simulation of a protein layer with different net charges per protein and (A) high relative permittivity (ε = 33) or (B) low relative permittivity (ε = 3.5). The other simulation conditions used are θ = 1, Γ_{max} = 4.4·10^{-8} mol·m^{-2}, c_w = 10 mM, and c_o = 10 mM. A pH value is not assigned since the charges are chosen to be permanent.

shifts the capacitance curve to more negative potentials. The shift is due to the fact that the protein actually has a positive charge in much of the potential window, therefore behaving as expected for a positive ion. This shift in net charge at the interface is caused by the low relative permittivity favoring the neutral form of amino acids, and since the pK_a values of the positive amino acids (lysine and arginine, pK_a ≈ 10.5 and 12.5) are more extreme than the negative (aspartate and glutamate, pK_a ≈ 4), this results in a shift toward a net positive charge. The simulation agrees well with the reported data on negative proteins which shift the pzc to negative potentials when measured at neutral pH. Further, this also explains why hemoglobin, considered a soft molecule, shifts the pzc to more negative values. We also notice that the value of the capacitance at the pzc is lowered for the soft proteins; this agrees with experimental observations in which the soft proteins insulin, glucose oxidase, bovine serum albumin, and hemoglobin all show lower capacitance at the pzc relative to the blank curve, compared to lysozyme and succinyl-lysozyme (see references in Table 1).

Differential Capacitance of Soft Proteins at Low Interfacial Charge. A second scheme in which the model predicts a global minimum found at opposite potentials than expected is found under conditions of low net charge and low relative permittivity of the protein. This situation is explored theoretically in Figure 9 for a protein which we assigned a set of different net charges at the interface and different relative permittivities.

The simulation results show that a global capacitance minimum that is not the pzc can theoretically be found for a protein layer at the ITIES if certain criteria are fulfilled: (1) a protein layer with low relative permittivity is formed at the interface and (2) the protein layer has a low charge per surface area. The position of this global minimum at more negative potentials corresponds well with that observed for the soft negatively charged proteins (see Table 1). This suggests that the observed minimum in these studies does not represent the actual pzc in the experiment.

The two scenarios presented here to explain the appearance of capacitance curves of soft proteins both require a low relative permittivity in the adsorbed layer and either a shift in net charge at the interface (Figure 8) or a low net charge at the interface (Figure 9). The observed minimum in experiments corresponds best with the situation of low charge at the interface (Figure 9) because the observed minimum is found at relatively extreme negative potentials. This suggests that this scenario is the most likely to explain the observed capacitance curves for soft proteins.

CONCLUSION

A computational model that evaluates the net charge of adsorbed proteins or other molecules as a consequence of charge regulation at the interface was developed. This was used to simulate experimentally obtained electrochemical capacitance responses for adsorption of proteins at the ITIES, which was in accordance with corresponding experimental data. We believe this can contribute to a better understanding of the mechanism behind electrochemical observations in such systems and of protein adsorption at liquid interfaces in general. It was found that the charge on the interface and on the adsorbing molecule itself may regulate the net charge through electrostatic interactions. This regulates the molecule toward a neutral charge, unless the influence of the surface charge is dominating, in which case the charge which is opposite of the surface is favored. The difference in relative permittivity at the interface, both from the properties of the interface itself and from a tendency of the protein to form dielectric layers at the interface, was also identified as key parameters in charge regulation. The protein layers formed at the interface correspond to a phase with a lower relative permittivity than the aqueous bulk phase; consequently, the neutral form of an ampholyte is predominant in the protein layer. In general the net charge of proteins is therefore lowered in the adsorbed layer as a result of charge regulation. In particular it was shown that charge regulation at the interface explains the unexpected shift in capacitance curves observed for some proteins, in particular negatively charged soft proteins. The unexpected shift is caused by charge regulation leading to one of two scenarios, (1) a shift of the net charge of the protein at the interface or (2) a global capacitance minimum, provoked by a low net charge at the interface, which may be falsely interpreted as the pzc. The latter possibility is in good accordance with experimentally observed capacitance curves.

dx.doi.org/10.1021/la204309a | *Langmuir* 2012, 28, 1804−1815

This work in which theory and experimental observations at ITIES are strongly correlated represents a new approach for future studies on protein adsorption at biomimetic interfaces. In a broader perspective, the present study is highly relevant for the understanding of protein structure and function in heterogeneous environments, which is relevant for the development of new protein based drug compounds.

■ ASSOCIATED CONTENT

Supporting Information

Detailed information on the calculation of the apparent pK_a from the relative permittivity and the electric potential at the interface. This material is available free of charge via the Internet at http://pubs.acs.org.

■ AUTHOR INFORMATION

Corresponding Author

*E-mail: hj@farma.ku.dk.

■ ACKNOWLEDGMENTS

The authors acknowledge the Faculty of Pharmaceutical Sciences, University of Copenhagen, for funding a "spirrekasse" project.

■ REFERENCES

(1) Pinholt, C.; Hartvig, R. A.; Medlicott, N. J.; Jorgensen, L. *Expert Opin. Drug. Deliv.* **2011**, 1−16.
(2) Arrigan, D. W. M. *Anal. Lett.* **2008**, *41*, 3233−3252.
(3) Dickinson, E. *Colloids Surf., B* **1999**, *15*, 161−176.
(4) Dickinson, E. *J. Chem. Soc., Faraday Trans.* **1998**, *94*, 1657−1669.
(5) Biesheuvel, P. M.; van der Veen, M.; Norde, W. *J. Phys. Chem. B* **2005**, *109*, 4172−4180.
(6) Santos, H. A.; Ferreira, E. S.; Pereira, E. J.; Pereira, C. M.; Kontturi, K.; Silva, F. *Chemphyschem* **2007**, *8*, 1540−1547.
(7) Lund, M.; Akesson, T.; Jonsson, B. *Langmuir* **2005**, *21*, 8385−8388.
(8) Hartvig, R. A.; van de Weert, M.; Ostergaard, J.; Jorgensen, L.; Jensen, H. *Langmuir* **2011**, *27*, 2634−2643.
(9) Stahlberg, J.; Jonsson, B. *Anal. Chem.* **1996**, *68*, 1536−1544.
(10) Pujar, N. S.; Zydney, A. L. *J. Colloid Interface Sci.* **1997**, *192*, 338−349.
(11) Zhao, X. L.; Subrahmanyan, S.; Eisenthal, K. B. *Chem. Phys. Lett.* **1990**, *171*, 558−562.
(12) Herzog, G.; Arrigan, D. W. M. *Analyst* **2007**, *132*, 615−632.
(13) Volkov, A. G.; Deamer, D. W.; Tanelian, D. L.; Markin, V. S. *Prog. Surf. Sci.* **1996**, *53*, 1−134.
(14) Santos, H. A.; Garcia-Morales, V.; Pereira, C. M. *Chemphyschem* **2010**, *11*, 28−41.
(15) Vanysek, P.; Sun, Z. *J. Electroanal. Chem.* **1990**, *298*, 177−194.
(16) Thomsen, A. E.; Jensen, H.; Jorgensen, L.; van de Weert, M.; Østergaard, J. *Colloids Surf., B* **2008**, *63*, 243−248.
(17) Herzog, G.; Moujahid, W.; Strutwolf, J.; Arrigan, D. W. M. *Analyst* **2009**, *134*, 1608−1613.
(18) Hartvig, R. A.; Méndez, M. A.; van de Weert, M.; Jorgensen, L.; Ostergaard, J.; Girault, H. H.; Jensen, H. *Anal. Chem.* **2010**, *82*, 7699−7705.
(19) Georganopoulou, D. G.; Williams, D. E.; Pereira, C. M.; Silva, F.; Su, T. J.; Lu, J. R. *Langmuir* **2003**, *19*, 4977−4984.
(20) Girault, H. H. J.; Schiffrin, D. J. *J. Electroanal. Chem.* **1984**, *179*, 277−284.
(21) Wandlowski, T.; Marecek, V.; Samec, Z. *J. Electroanal. Chem.* **1988**, *242*, 277−290.
(22) Kakiuchi, T.; Kondo, T.; Kotani, M.; Senda, M. *Langmuir* **1992**, *8*, 169−175.
(23) Roozeman, R. J.; Murtomaki, L.; Kontturi, K. *J. Electroanal. Chem.* **2005**, *575*, 9−17.
(24) Collins, C. J.; Lyons, C.; Strutwolf, J.; Arrigan, D. W. M. *Talanta* **2010**, *80*, 1993−1998.
(25) Scanlon, M. D.; Jennings, E.; Arrigan, D. W. M. *Phys. Chem. Chem. Phys.* **2009**, *11*, 2272−2280.
(26) Kivlehan, F.; Lanyon, Y. H.; Arrigan, D. W. M. *Langmuir* **2008**, *24*, 9876−9882.
(27) Herzog, G.; Kam, V.; Arrigan, D. W. M. *Electrochim. Acta* **2008**, *53*, 7204−7209.
(28) Vanysek, P.; Reid, J. D.; Buck, R. P. *J. Electrochem. Soc.* **1984**, *131*, C107.
(29) Vagin, M. Y.; Trashin, S. A.; Ozkan, S. Z.; Karpachova, G. P.; Karyakin, A. A. *J. Electroanal. Chem.* **2005**, *584*, 110−116.
(30) Herzog, G.; Nolan, M. T.; Arrigan, D. W. M. *Electrochem. Commun.* **2011**, *13*, 723−725.
(31) Su, B.; Eugster, N.; Girault, H. H. *J. Electroanal. Chem.* **2005**, *577*, 187−196.
(32) Mendez, M. A.; Su, B.; Girault, H. H. *J. Electroanal. Chem.* **2009**, *634*, 82−89.
(33) Santos, H. A.; Chirea, M.; García-Morales, V.; Silva, F.; Manzanares, J. A.; Kontturi, K. *J. Phys. Chem. B* **2005**, *109*, 20105−20114.
(34) van der Veen, M.; Norde, W.; Stuart, M. C. *Colloids Surf., B* **2004**, *35*, 33−40.
(35) Girault, H. H. J.; Schiffrin, D. J. *Electrochim. Acta* **1986**, *31*, 1341−1342.
(36) Slevin, C. J.; Malkia, A.; Liljeroth, P.; Toiminen, M.; Kontturi, K. *Langmuir* **2003**, *19*, 1287−1294.
(37) Cho, D. *J. Ind. Eng. Chem.* **2000**, *6*, 325−330.
(38) Fernandez, M. S.; Fromherz, P. *J. Phys. Chem.* **1977**, *81*, 1755−1761.
(39) Wang, H. F.; Borguet, E.; Eisenthal, K. B. *J. Phys. Chem. B* **1998**, *102*, 4927−4932.
(40) Matyushov, D. V.; Schmid, R.; Ladanyi, B. M. *J. Phys. Chem. B* **1997**, *101*, 1035−1050.
(41) Iwunze, M. O. *Phys. Chem. Liq.* **2005**, *43*, 195−203.
(42) Yufei, C.; Cunnane, V. J.; Schiffrin, D. J.; Murtomaki, L.; Kontturi, K. *J. Chem. Soc., Faraday Trans.* **1991**, *87*, 107−114.
(43) Gilson, M. K.; Honig, B. H. *Biopolymers* **1986**, *25*, 2097−2119.
(44) Liljeroth, P.; Malkia, A.; Cunnane, V. J.; Kontturi, A. K.; Kontturi, K. *Langmuir* **2000**, *16*, 6667−6673.
(45) Martins, M. C.; Pereira, C. M.; Santos, H. A.; Dabirian, R.; Silva, F.; Garcia-Morales, V.; Manzanares, J. A. *J. Electroanal. Chem.* **2007**, *599*, 367−375.
(46) Beverung, C. J.; Radke, C. J.; Blanch, H. W. *Biophys. Chem.* **1999**, *81*, 59−80.
(47) Kleijn, M.; Norde, W. *Heterogen. Chem. Rev.* **1995**, *2*, 157−172.
(48) Norde, W. *Adv. Colloid Interf. Sci.* **1986**, *25*, 267−340.
(49) Martin, A. H.; Stuart, M. A. C.; Bos, M. A.; van Vliet, T. *Langmuir* **2005**, *21*, 4083−4089.
(50) Atkinson, P. J.; Dickinson, E.; Horne, D. S.; Richardson, R. M. *J. Chem. Soc., Faraday Trans.* **1995**, *91*, 2847−2854.
(51) Postel, C.; Abillon, O.; Desbat, B. *J. Colloid Interface Sci.* **2003**, *266*, 74−81.
(52) Eaglesham, A.; Herrington, T. M.; Penfold, J. *Colloids Surf.* **1992**, *65*, 9−16.
(53) Dickinson, E.; Horne, D. S.; Phipps, J. S.; Richardson, R. M. *Langmuir* **1993**, *9*, 242−248.
(54) Stelzle, M.; Sackmann, E. *Biochim. Biophys. Acta* **1989**, *981*, 135−142.
(55) More, S. D.; Hudecek, J.; Urisu, T. *Surf. Sci.* **2003**, *532−535*, 993−998.
(56) Kuramitsu, S.; Hamaguchi, K. *J. Biochem.* **1980**, *87*, 1215−1219.
(57) van der Veen, M.; Stuart, M. C.; Norde, W. *Colloids Surf., B* **2007**, *54*, 136−142.
(58) Girault, H. H. *Analytical and Physical Electrochemistry*, 1st ed.; EPFL Press: Lausanne, Switzerland, 2004.
(59) van der Veen, M.; Norde, W.; Stuart, M. C. *J. Agric. Food Chem.* **2005**, *53*, 5702−5707.
(60) Yang, A. S.; Honig, B. *J. Mol. Biol.* **1993**, *231*, 459−474.

(61) Kowalska, A.; Gyugos, M.; Szego, D.; Pineda, A. L.; Ayala, D.; Xu, Y.; Hughes, N.; Tito, A.; Jablonska, J. *Food Chem. Biotech.* **2007**, *71*, 35.
(62) Kosa, T.; Maruyama, T.; Otagiri, M. *Pharm. Res.* **1998**, *15*, 449–454.